

Gamma-Ray Spectrometric Determination of Burnup Distribution and Cooling Time of Spent PWR Fuel Assemblies

Young-Gil Lee

Korea Advanced Energy Research Institute

Jae-Shik Jun

Chungnam National University

(Received August 21, 1984)

감마선 분광분석에 의한 조사후 핵연료 집합체(PWR)의 연소분포 및 냉각시간 결정

이 영 길

한국에너지연구소

전 재 식

충남대학교

(1984. 8. 21 접수)

Abstract

Non-destructive gamma-ray spectrometry was carried out on the spent PWR fuel assemblies at the spent fuel pool of reactor-site. Attention was focused on the determination of burnup distribution and cooling time. For the measurement of burnup distribution, the concentration ratio of $^{134}\text{Cs}/^{137}\text{Cs}$ was used and the results showed these ratios varied with the positions of assemblies in the core during their irradiation. For the measurement of cooling time, $^{144}\text{Ce}/^{137}\text{Cs}$ was used and the results were agreed considerably well with the operator declared cooling time.

요 약

원자력 발전소의 조사후 핵연료 저장물에서 조사후 핵연료 집합체에 대한 감마선 분광분석 실험을 비파괴적인 방법으로 수행하였다. 조사후 핵연료 집합체가 갖는 연소분포를 알기 위해서 1차핵분열 생성물과 2차핵분열 생성물간의 감마선 강도비인 $^{134}\text{Cs}/^{137}\text{Cs}$ 를 사용했으며 그 결과는 이들 집합체가 노심내에서 연소시에 가졌던 중성자 분포의 기대치와 상응하였다. 이로부터 감마선 강도비 $^{134}\text{Cs}/^{137}\text{Cs}$ 은 연소도 해석을 위한 좋은 인디케이터임을 확인하였다. 핵물질의 안전관리면에서 중요시되고 있는 조사후 핵연료의 냉각시간을 감마선 강도비 $^{144}\text{Ce}/^{137}\text{Cs}$ 를 사용하여 구했으며 이를 핵연료 관리기록에 의한 냉각시간과 비교해 본 결과 각각 2%, 10%이내의 차이를 나타내었다. 이로부터 본 실험에서 냉각시간을 구하기 위해서 유도한 방정식을 단일 주기로 연소된 핵연료에 대해서 사용할 수 있음을 실증하였다.

I. Introduction

Gamma-ray spectrometric studies of nuclear

fuel began in the end of 1960s. In the beginning, the experiments were mainly carried out on spent fuel rods or samples.¹⁻⁵⁾ For last

several years, however, non-destructive gamma-ray spectrometric measurement on an extensive scale has been under development in many advanced countries because the spectrometry on spent nuclear fuel assemblies is one of the very important methods in particular for the evaluation of burnt-up fuel.⁶⁻¹⁰⁾

In order to develop and improve the technique of the non-destructive evaluation of spent nuclear fuel assemblies discharged from the power reactor, high resolution gamma-ray spectrometric experiment was performed on spent nuclear fuel assemblies at the spent pool of Mihama-3 PWR as a joint research program between Japan Atomic Energy Research Institute (JAERI) and Kansai Electric Power Company.⁶⁾

Two assemblies with different irradiation histories were selected for the experiment, and the data acquired during the measurement were analyzed for the determination of burnup distribution and cooling time.

For the analysis of burnup distribution, the gamma-ray intensity ratio of secondary fission product to direct fission product was used because it is directly proportional to the integrated neutron flux which is in turn proportional to burnup. The gamma-ray intensity ratio of direct fission products with sufficiently different half lives could be used for the estimation of cooling time, and this estimation was necessary both for safeguards and as initial information in the burnup measurement.

II. Theory

II-1. Relative Burnup Distribution

If the neutron flux in the core is constant during irradiation and the half-lives of the fission products are relatively long compared with the irradiation time, the activity from a direct fission product A_d (such as ^{106}Ru or ^{137}Cs) and that from a nuclide formed by neutron capture of the direct fission product A_s (such as

^{134}Cs or ^{154}Eu) can be represented by the following equations.

$$A_d \propto \Sigma_f \cdot (\phi \cdot T) \quad (1)$$

$$A_s \propto \Sigma_f \cdot \sigma(n, \gamma) \cdot (\phi \cdot T)^2 \quad (2)$$

where

Σ_f : spectrum & time averaged fission cross section,

ϕ : spectrum & time averaged neutron flux,

T : irradiation time,

$\sigma(n, \gamma)$: spectrum & time averaged neutron capture cross section of direct fission product.

Eqs. (1) and (2) show that the activity ratio A_s/A_d is also proportional to $(\phi \cdot T)$, namely,

$$A_s/A_d \propto (\phi \cdot T) \quad (3)$$

and Eq. (3) can be used as a burnup monitor in principle.^{6, 11-14)}

The main advantage of the activity ratio method in gamma-ray spectrometry is that the only necessary parameter is relative detection efficiency of the detector used instead of absolute detection efficiency which must be known for absolute activity measurement. Moreover, the former is less sensitive to the variation of geometry than the latter.^{12, 15)}

II-2. Cooling Time

The activity ratio of direct fission products with sufficiently different half-lives, such as $^{144}\text{Ce}/^{137}\text{Cs}$, can be used as a cooling time monitor for irradiated nuclear fuel.¹⁶⁻¹⁹⁾ To derive the cooling time equation as a function of detected gamma-ray intensity ratio of direct fission products instead of activity ratio, the following steps are necessary.

The gamma-ray activities A_1 and A_2 of two nuclides 1 and 2, respectively, are expressed by the following equations.

$$A_1 = A_1^0 \times e^{-\lambda_1 \cdot T} \quad (4)$$

$$A_2 = A_2^0 \times e^{-\lambda_2 \cdot T} \quad (5)$$

where

A_1^0, A_2^0 : activities at shut-down,

λ_1, λ_2 : decay constants,

T_c : cooling time.

Dividing Eq. (5) by Eq. (4) gives

$$T_c = \frac{1}{\lambda_2 - \lambda_1} \times \ln \left(\frac{A_1}{A_2} \times \frac{A_2^0}{A_1^0} \right). \quad (6)$$

The activity ratio A_1/A_2 in Eq. (6) is given by

$$\frac{A_1}{A_2} = \frac{I_1^i}{I_2^j} \times \frac{BR_2^j}{BR_1^i} \times \frac{E_2^j}{E_1^i} \quad (7)$$

where

I_1^i, I_2^j : detected intensities of gamma-ray energies i and j ,

BR_1^i, BR_2^j : branching ratios,

E_1^i, E_2^j : absolute detection efficiencies.

By assuming that the fuel assemblies selected for the measurement were irradiated under a constant power level in the core and the depletion of the generated fission products was only possible by radioactive decay, the activity ratio A_2^0/A_1^0 in Eq. (6) is also given by

$$\frac{A_2^0}{A_1^0} = \frac{Y_2}{Y_1} \times \frac{1 - e^{-\lambda_2 \cdot T}}{1 - e^{-\lambda_1 \cdot T}} \quad (8)$$

where

Y_1, Y_2 : fission yields of two nuclides 1 and 2,

T : irradiation time.

Finally, substituting Eqs. (7) and (8) into Eq. (6), the cooling time equation is presented as a function of detected gamma-ray intensity ratio.¹⁷⁾

$$T_c = \frac{1}{\lambda_2 - \lambda_1} \cdot \ln \left(\frac{I_1^i}{I_2^j} \cdot \frac{BR_2^j}{BR_1^i} \cdot \frac{E_2^j}{E_1^i} \cdot \frac{Y_2}{Y_1} \cdot \frac{1 - e^{-\lambda_2 \cdot T}}{1 - e^{-\lambda_1 \cdot T}} \right). \quad (9)$$

In order to determine the relative detection efficiency, E_2^j/E_1^i , of two gamma-ray energies i and j in Eq. (9), the curve of relative detection efficiency of a given energy interval of the spectrum must be given. Several pronounced and well resolved lines of the radioisotope in the spectrum are used because the relative detection efficiency of this radioisotope has the following expression.

$$\frac{E^l}{E^m} = \frac{BR^m \times I^l}{BR^l \times I^m} \quad (10)$$

where

E^l, E^m : absolute detection efficiencies of

gamma-ray energies l and m ,

BR^l, BR^m : branching ratios,

I^l, I^m : detected gamma-ray intensities.

This relative detection efficiency depends on several non-linear factors and it is difficult to predict the efficiency by a theoretical approach. But, the experimental curve of relative detection efficiency using the measured relative detection efficiencies can be obtained as a function of energy because the absolute detection efficiencies E^l and E^m have the same geometrical factors.

III. Experiment

III-1. Experimental Set-Up

The gamma-ray spectrometric experiment were carried out on spent nuclear fuel assemblies (PWR 15×15) immersed in the spent fuel pool of Mihama-3 pressurized water reactor. Fig. 1 shows the schematic core map of the Mihama-3 reactor and the positions of assemblies A-27 (1st cycle) and D-14 (2nd cycle) which were selected for the measurement.

The geometry for spent fuel assembly measurement in the pool was to isolate an assembly from other irradiated assemblies and to guide gamma-rays from the spent fuel assembly under consideration to the detector located at the edge of the spent fuel pool. A simplified sketch of

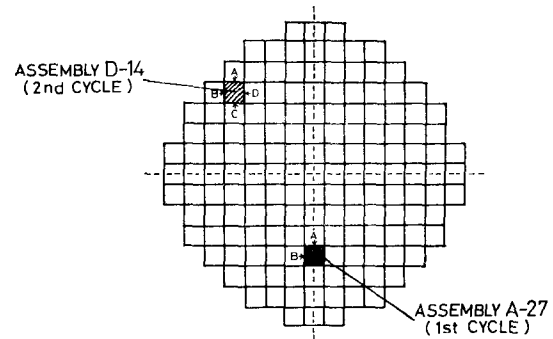


Fig. 1. Schematic Core Map of Mihama-3PWR and the Positions of Assemblies A-27 and D-14

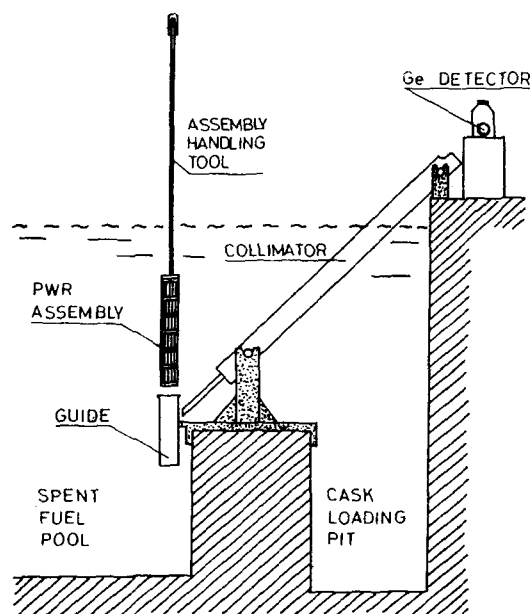


Fig. 2. The Set-up for Gamma-ray Spectrometry at Spent Fuel Pool of Mihama-3 PWR

the equipment set-up is shown in Fig. 2. A gamma-ray collimator, 13.8 meters in length, was used as an air channel in the water and its immersion angle was 45 degrees. It was sustained by two poles; one immersed in the pool and another installed at the edge of the pool.

Two types of measurement named "Diagonal measurement" and "Side measurement" were performed in consideration of their individual advantages and particular characteristics.^{7,20)}

III-2. Gamma-Ray Spectrometry

The system of gamma-ray spectrometry used for the experiment consisted of a high purity Ge detector, a pre-amplifier, a high voltage source, an amplifier, a multichannel analyzer and a mini computer with recording devices.

The positions of an assembly at which gamma-ray spectrometry was carried out had been decided after obtaining the spectrum of gamma-ray scanning on the assembly. 7 axial positions in one side (or diagonal) were selected as the measuring points, and these positions were

located between grids to avoid the influence of gamma-ray coming from grid.

The obtained gamma-ray spectra were analyzed by means of "GAMMA-3" computer program stored in a portable mini computer. The energy range of measurement was set between 300 keV and 2,400 keV because it includes the most intensive gamma-ray lines of ^{106}Ru , ^{134}Cs , ^{137}Cs , ^{144}Ce and ^{154}Eu which are measurable fission products even after a long time cooling.

IV. Results and Discussion

IV-1. Relative Burnup Distribution

Fig. 3 represents the relative burnup distribution of assembly A-27 along its axial direction in terms of the gamma-ray intensity ratio $^{134}\text{Cs}/^{137}\text{Cs}$. This figure shows that the burnup distributions of measured sides A and B of assembly A-27 were near coincident and the central region of fuel assembly had much higher burnup than those of both ends. The close coincidence of burnup distributions of two sides A and B are considered as the results of the small differences in neutron flux and spectra at sides A and B of assembly A-27 during irradiation.

Fig. 4 is the result of the side measurement

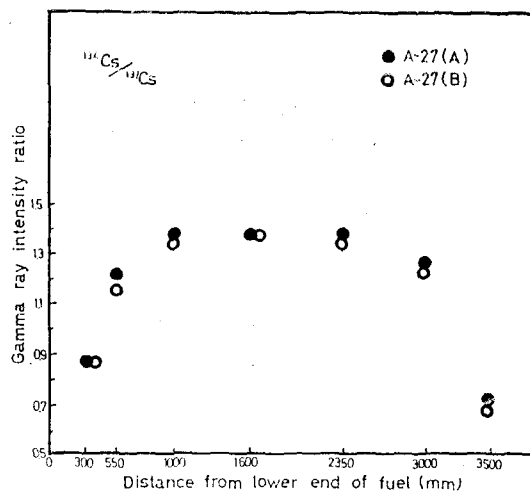


Fig. 3. Relative Burnup Distributions of Assembly A-27

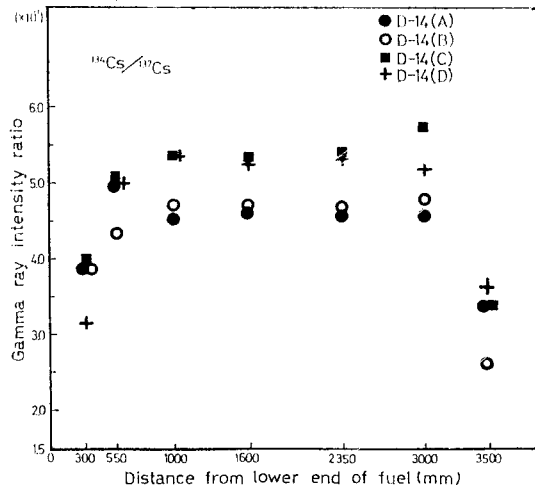


Fig. 4. Relative Burnup Distributions of Assembly D-14 (Side)

of assembly D-14, and Fig. 5 shows the result of the diagonal measurement of the same assembly. From these two figures, it is possible to find that the burnup of sides C and D were markedly higher than those of sides A and B, and the burnup distributions along the axial direction of this assembly had plateaus. The phenomena of the differences in burnup can be explained by considering that the sides C and D looked out on the central core had the higher neutron flux than those of sides A and B which were faced to the periphery of the core (see Fig. 1). From the shapes of relative burnup distributions of assemblies A-27 and D-14, it will be possible to conjecture the profiles of neutron flux during the first and the second

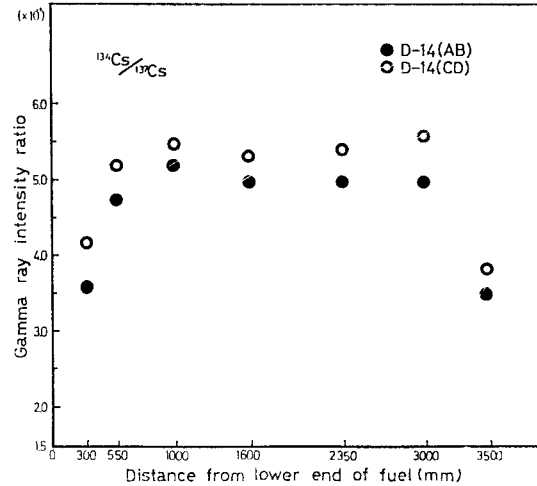


Fig. 5. Relative Burnup Distributions of Assembly D-14 (Diagonal)

cycles.

IV-2. Cooling Time

Based on the intensity ratios of direct fission products ^{144}Ce (1,489 keV)/ ^{137}Cs (662 keV) and the data given in Table 1, the cooling time were calculated. To get the relative detection efficiencies given in the Table 1, the gamma-ray peaks of three nuclides ^{106}Ru , ^{134}Cs and ^{144}Ce in the gamma-ray spectrum were chosen. The detection efficiency of 1,365 keV gamma-ray energy of ^{134}Cs was taken as unit value 1, then normalized the curve of other gamma-ray detection efficiencies to that of ^{134}Cs at 1,365 keV.

Table 2 shows that the measured cooling time of assembly A-27 was 41.5 months, and those of assembly D-14 were 32.2 months (side

Table 1. The Data Used for Cooling Time Calculation

Nuclide (γ -ray energy; keV)	Decay constant λ (1/day)	Relative detection efficiency ϵ	Branching ratio BR (%)	Fission yield Y (%)	Irradiation time T (day)
^{137}Cs (661.60)	6.293×10^{-5}	* 0.324 # 0.476 & 0.461	85.10	6.20	584
^{144}Ce (1489.12)	2.440×10^{-3}	* 1.055 # 1.046 & 1.060	0.29	5.40	230

* Assembly A-27 # Assembly D-14 (side measurement) & Assembly D-14 (diagonal measurement)

Table 2. The Measured Cooling Times

Position	A-27			D-14 (Side)					D-14 (Diagonal)		
	A	B	A verage	A	B	C	D	A verage	AB	CD	A verage
1	40.7	40.1	40.4	31.6	33.0	32.8	33.3	32.7	31.5	31.5	31.5
2	41.4	41.6	41.5	32.2	33.3	33.1	31.5	32.5	30.5	30.8	30.7
3	41.7	41.6	41.7	31.5	32.1	32.5	32.8	32.2	30.8	32.5	31.7
4	43.8	42.7	43.3	32.6	33.3	31.4	31.6	32.2	30.6	31.4	31.0
5	41.3	41.9	41.6	33.4	31.0	32.7	31.3	32.1	30.9	31.3	31.1
6	41.9	40.6	41.3	32.7	31.7	32.2	—	32.2	30.9	31.5	31.2
7	39.9	41.2	40.6	31.7	31.1	31.6	31.6	31.5	30.4	31.3	30.9
Average	41.5	41.4	41.5 months	32.2	32.2	32.3	32.0	32.2 months	30.8	31.5	31.1 months
Operator declared cooling time	41.1 months			29.2 months					29.4 months		
Mean difference	1.9%			10.2%					5.8%		

measurement) and 31.1 months (diagonal measurement), respectively.

Comparison of the measured cooling times with the operator declared cooling times shows satisfactory agreement with mean differences of 1.9% (A-27), 10.2% (D-14, side) and 5.8% (D-14, diagonal). And consequently it seems that the Eq. (9) is suitable for the estimation of cooling time, should we assume the nuclear fuel was exposed under a constant power level as well as the fission products depleted by radioactive decay only.

From the agreement of the measured cooling times with the operator declared cooling times, it is possible to corroborate that the measured relative detection efficiencies were well and reasonably calculated.

For the cooling time analysis, it was possible to simplify the power levels during the irradiation of assemblies A-27 and D-14 because these two assemblies were exposed only during one cycle (A-27: 1st cycle, D-14: 2nd cycle), but in the case of several cycle irradiation it is not possible to simplify the power level and more elaborate method will be required for the calculation of cooling time.

V. Conclusions

The burnup distribution analysis of spent nuclear fuel assemblies could be possible by the measurement of the intensity ratio of $^{134}\text{Cs}/^{137}\text{Cs}$. And this intensity ratio is currently considered as a good indicator of burnup. It was found that intensity ratios corresponding to a given burnup distribution varied with the positions of assemblies in the core during their irradiation. This variation could be explained by introducing the spatial variations of the neutron spectrum during the reactor operation.

The measured cooling times were in good agreement with the operator declared cooling times, and consequently the Eq. (9) is turned out to be suitable for the estimation and verification of cooling time if it is possible to assume that the nuclear fuel was irradiated under a constant power level as well as the fission products were depleted by radioactive decay only.

Acknowledgements

The authors wish to express their gratitude to Dr. I. Kobayashi of JAERI and the author-

ities of JAERI for their sincere encouragement to carry out this work.

References

1. M.F. Banham et al., AERE-R 5864 (1968).
2. D.G. Boase et al., AECL-3952 (1971).
3. M.F. Banham et al., "Application of High Resolution Gamma-ray Spectrometry in the Post-irradiation Examination of Nuclear Fuel Materials", B.N.E.S. (1972).
4. R.S. Forsyth et al., IAEA-SM-133/4 (1970).
5. J.M. Butterfield et al., CEGB/RD/B/N2069 (1971).
6. 鶴田晴通, 晴木功, 三好慶典, 李榮吉, JAERI-memo-9521 (1981).
7. G. Adiletta et al., EUR 5289e (1974).
8. M.L. Pointud et al., PI/SED TI/300/544/80, C.E.A-C.E.N.G (1980).
9. J.R. Phillips et al., LA-8212 (1980).
10. G.L. Hanna, ASO/R2, R3 (1978).
11. J.D. Chen et al., AECL-6192 (1978).
12. S.T. Hsue, Atom. Energ. Rev. **161** 89 (1978).
13. R. John et al., Nucl. Tech. **46**, 21 (1979).
14. C. Foggi et al., CEC, ICT-21 (1978).
15. S.T. Hsue et al., LA-6923 (1978).
16. I. Ursu et al., IAEA-SM-201/86 (1976).
17. H. Graber et al., IAEA-SM-231/129 (1979).
18. T. Dragnev et al., EUR-4576e (1971).
19. G.L. Hanna, IAEA-SM-231/132 (1979).
20. A.M. Bresesti et al., EUR-5334e (1975).